

XAFS theory studied by closed-path Green's function

Takashi Fujikawa

Graduate School for Science, Chiba University, Yayoi-cho 1-33, Inage, Chiba 263-8522, Japan.
E-mail: fujikawa@scichem.s.chiba-u.ac.jp

The basic framework of X-ray absorption fine structure (XAFS) theory is formulated by use of the non-equilibrium Keldysh–Green function, which presents a unified view of XAFS spectra at zero and nonzero temperature. In particular, the relation between the scattering Green's function and the retarded Green's function G^r is discussed, along with resonance effects in XAFS. The latter effects give rise to unexpected peaks within one-electron theory. Loss effects, both intrinsic and extrinsic, are also discussed.

Keywords: Keldysh–Green function; resonance effects; many-body effects.

1. Introduction

XAFS theory has been developed on the basis of scattering theory. The highly successful standard XAFS analysis programs *FEFF*, developed by Rehr *et al.* (1991), and *EXCURVE*, developed by Binsted & Hasnain (1996), are based on the cluster- and multiple-scattering approach (for example, see, Lee & Pendry, 1975). The basic theoretical framework, starting from many-body scattering theory, has been presented by Hedin, employing the quasi-boson approximation (Hedin, 1989). More sophisticated formulae, beyond the quasi-boson approximation, have been obtained by the present author (Fujikawa, 1999). These scattering theories, based on projection-operator techniques, have proven to be very powerful; however, it is difficult to include the effects of temperature on XAFS analyses because the quantum state to be projected onto and out of has to be specified. In some special cases, the thermal average may be taken to include the temperature effects. For example, Debye–Waller and Franck–Condon factors in single-scattering EXAFS analyses can simultaneously be included within the harmonic approximation for nuclear vibration (Fujikawa, 1996a,b). It is, however, difficult to go beyond the harmonic approximation or the single-scattering approximation.

A different approach, starting from the non-equilibrium Green's function, has also been developed by the present author, in order to discuss finite temperature XAFS spectra (Fujikawa, 1999). It is possible to obtain a systematic approximation for the XAFS analyses at $T = 0$ and $T > 0$. In the previous paper (Fujikawa, 1999), some important problems, such as the Debye–Waller and Franck–Condon factors, and the subtle cancellation of loss structures, were discussed. In this paper, a further discussion is presented on the relation between the scattering Green's function and the retarded Green's function G^r , as well as on the resonance effects in XAFS. To date, these problems have rarely been discussed.

2. Closed-path Green's function XAFS formulae

In this paper, the closed-path (Keldysh) Green function is extensively used to describe the X-ray absorption intensity. In dipole length and acceleration form, the X-ray absorption intensity $I(\omega)$ for an X-ray photon of energy ω is (Fujikawa, 1999)

$$I(\omega) = i \int dx dx' \Delta^*(x) \Delta(x') \int_{-\infty}^{\infty} \pi^>(xt, x') \exp(i\omega t) dt, \quad (1)$$

where $x = (\mathbf{r}, \sigma)$ and $\pi^>$ is the reducible polarization propagator defined by $i\pi^>(1, 2) = \langle \delta\rho(1)\delta\rho(2) \rangle [\delta\rho(1) = \rho(1) - \langle \rho(1) \rangle]$. In the dipole-length formula, we have $\Delta \propto \mathbf{e} \cdot \mathbf{r}$ for linear polarization, where \mathbf{e} is the polarization vector of the incident X-ray.

It is not easy to handle the reducible polarization propagator π , so we relate it to the irreducible polarization propagator P and the screened Coulomb interaction W :

$$\pi(1, 2) = P(1, 2) + \int d3 d4 P(1, 3)W(3, 4)P(4, 2). \quad (2)$$

Note that only the greater ($>$) part of π is needed.

To obtain a realistic and useful approximation, a skeleton expansion of P is applied, *i.e.* expansion in terms of full G keeping all interactions other than electron–photon interactions.

3. The lowest-order approximation in skeleton expansion

The lowest-order term, the skeleton bubble (see Fig. 1a) for P in the first term of (2), is given by

$$iP^>(xt, x') \simeq G^>(xt, x')G^<(x', xt). \quad (3)$$

The greater Green's function, $G^>$, describes the propagation of excited electrons and the lesser Green's function, $G^<$, describes the occupied bound states from which electrons are excited.

In the core-excitation processes, $G^<$ is well approximated by

$$iG^<(x', xt) \simeq -\varphi_c^*(x)\varphi_c(x')\langle b^\dagger(t)b \rangle, \quad (4)$$

where $b(b^\dagger)$ is the annihilation (creation) operator associated with the core state φ_c . Substituting (4) into (3), the lowest-order term of the X-ray absorption intensity $I(\omega)$ in the skeleton expansion can be written as

$$I^{(0)}(\omega) = \int (d\varepsilon/2\pi) G_{XA}^>(\varepsilon) G_c^<(\varepsilon - \omega), \quad (5)$$

where

$$G_{XA}^>(\varepsilon) = i \int dx dx' \Delta^*(x) \Delta(x') G^>(x, x'; \varepsilon) \varphi_c^*(x) \varphi_c(x') \quad (6)$$

and

$$G_c^<(\omega) = \int \langle b^\dagger(t)b \rangle \exp(-i\omega t) dt. \quad (7)$$

Both $G_{XA}^>$ and $G_c^<$ have transparent physical meanings. $G_{XA}^>$ describes the X-ray absorption processes without core-hole effects, whereas $G_c^<$ describes the core effects and shake effects (intrinsic effect).

To understand the physics involved in $G_{XA}^>$ and $G_c^<$, we shall consider an explicit expression for $I^{(0)}(\omega)$ at 0 K in terms of Dyson orbitals defined by (Hedin & Lundqvist, 1969)

$$\begin{aligned} g_n(x) &= \langle n, N-1 | \psi(x) | 0, N \rangle, \\ \varepsilon_n &= E_0(N) - E_n(N-1), \\ f_p(x) &= \langle 0, N | \psi(x) | p, N+1 \rangle, \\ \varepsilon_p &= E_p(N+1) - E_0(N), \end{aligned} \quad (8)$$

where $|0, N\rangle$ is the ground state of an N -electron system and $\psi(x)$ is the field operator. The explicit formulae of $G^>$ and $G^<$ in terms of the Dyson orbitals are

$$iG^>(x, x'; \omega) = 2\pi \sum_p f_p(x) f_p^*(x') \delta(\omega - \varepsilon_p) \quad (9)$$

and

$$iG^<(x', x; \omega) = -2\pi \sum_n g_n(x') g_n^*(x) \delta(\omega - \varepsilon_n). \quad (10)$$

The retarded Green's function G^r has a spectral representation:

$$G^r(x, x'; \varepsilon) = \sum_p \frac{f_p(x)f_p^*(x')}{\varepsilon - \varepsilon_p + i\eta} + \sum_n \frac{g_n(x)g_n^*(x')}{\varepsilon - \varepsilon_n + i\eta}. \quad (11)$$

The substitution of (9) into (6) yields

$$G_{XA}^>(\varepsilon) = 2\pi \sum_p |f_p|\Delta|\phi_c\rangle|^2 \delta(\varepsilon - \varepsilon_p). \quad (12)$$

This is positive so that $G_{XA}^>(\varepsilon)$ can also be written as

$$G_{XA}^>(\varepsilon) = -\text{Im}\langle c|\Delta^*G^>(\varepsilon)\Delta|c\rangle. \quad (13)$$

In the X-ray absorption process, if the condition $\varepsilon \gg \mu$ is satisfied, the second term of (11) can be neglected because of the large energy denominator. In this case

$$G_{XA}^>(\varepsilon) \simeq -2\text{Im}\langle c|\Delta^*G^r(\varepsilon)\Delta|c\rangle. \quad (14)$$

Note the factor 2 in equation (14), in contrast to equation (13). As the sum over p in equation (9) runs over both the bound and continuum states, both equation (13) and equation (14) can describe the pre-edge structures and also the X-ray absorption near-edge structure (XANES) above the ionization edge.

The expression (13) for $G_{XA}^>(\varepsilon)$ in terms of $G^>$ is useful in the case where ε is close to the core threshold, because we can use a formula for $G^>$ in terms of the Fermi distribution function $f(\varepsilon)$ and the spectral function $A(\varepsilon)$:

$$iG^>(\varepsilon) = [1 - f(\varepsilon)]A(\varepsilon). \quad (15)$$

Substituting (15) into (13), we obtain an interesting formula for $G_{XA}^>(\varepsilon)$:

$$G_{XA}^>(\varepsilon) = -[1 - f(\varepsilon)]\text{Im}\langle c|\Delta^*A(\varepsilon)\Delta|c\rangle. \quad (16)$$

The factor $1 - f(\varepsilon)$ prohibits the transition to the 'occupied' states. It is interesting to note that the one-electron-like factor $1 - f(\varepsilon)$ enters the correlated many-body expression without further approximation. As far as it is possible to calculate the spectral function $A(\varepsilon)[1 - f(\varepsilon)]$ by using conventional molecular-orbital or band-calculation techniques, we obtain the 'lowest-order' X-ray absorption intensity.

The difficult problem remains, however, of how to obtain $A(\varepsilon)$ for the highly excited states. However, G^r offers some advantages for XAFS analysis because G^r satisfies the closed Dyson equation, and may be used instead of the complicated Keldysh equation for $G^>$:

$$G^r = G_0^r + G_0^r \Sigma^r G^r. \quad (17)$$

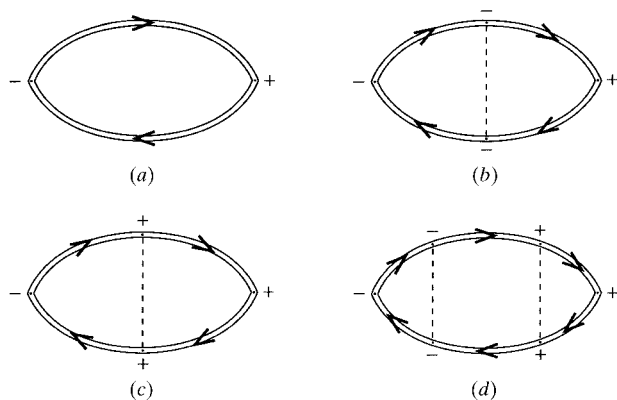


Figure 1
(a) The lowest-order skeleton Keldysh diagram for the X-ray absorption intensity. (b), (c), (d) The resonance Keldysh diagrams. Coulomb lines are connected to the same time leg.

The self-energy (optical potential) Σ^r is conveniently calculated by use of the analytical continuation technique from Σ for the imaginary time representation, that is, $i\omega_n$ in Σ is replaced by $\omega - i\eta$, which yields Σ^r (Mahan, 1990). The temperature effects can be taken into account in Σ^r ; on the other hand, it is difficult to include the core-hole effects in the Σ^r calculation. For the latter purpose, the many-body scattering approach is much better (Hedin, 1989; Fujikawa, 1999).

Neglecting phonon effects, an expression of $G_c^<$ in terms of the intrinsic amplitude S_n , defined by $S_n = \langle n, N - 1|b|0, N\rangle$, can be obtained:

$$G_c^<(\omega) = 2\pi \sum_n |S_n|^2 \delta(\omega - \varepsilon_n). \quad (18)$$

From equations (5), (14) and (18), we thus obtain the X-ray absorption intensity within the intrinsic approximation:

$$I^{(0)}(\omega) = -2 \sum_n |S_n|^2 \text{Im}\langle c|\Delta^*G^r(\omega + \varepsilon_n)\Delta|c\rangle. \quad (19)$$

When G^r is replaced by the corresponding scattering Green's function, this expression is a well known XAFS formula that only considers shake-up and shake-off loss processes (Rehr *et al.*, 1978).

Phonon effects can be discussed within the present theoretical framework. When we use the approximation (14) for $G_{XA}^>$, we first obtain the usual XAFS formulae and next average them over phonon states at finite temperature. This two-step calculation is legitimate as far as electron-phonon interactions are neglected and yields the Debye-Waller factors. For $G_c^<$, we have to include the phonon effects in the operator $b^\dagger(t) = \exp(iHt)b^\dagger \exp(-iHt)$ in equation (7), where the Hamiltonian H has the phonon part before and after the core-hole production. Therefore, $G_c^<$ can describe the Franck-Condon factors. The X-ray absorption intensity is written as the convolution product of these two factors (Fujikawa, 1999).

4. Resonance effects in XAFS

So far, resonance effects in XAFS have not been discussed in detail. Here they are discussed based on the Keldysh-Green function formalism. Figs. 1(b), 1(c) and 1(d) show the resonance Keldysh diagrams, while Figs. 1(a) is the lowest-order diagram, as discussed in the previous section. Figs. 1(b) and 1(c) give the X-ray absorption intensity in terms of the Dyson orbitals defined by equation (8):

$$I^{(b)}(\omega) + I^{(c)}(\omega) = 2\pi \text{Re} \sum_{np} \sum_{mq} \left[\langle g_n|\Delta^*|f_p\rangle \times \left(\frac{\langle f_q f_p|g_n g_m\rangle \langle g_m|\Delta|f_q\rangle}{\omega + \varepsilon_q - \varepsilon_m - i\eta} - \frac{\langle g_m f_p|g_n f_q\rangle \langle f_q|\Delta|g_m\rangle}{\omega - \varepsilon_q + \varepsilon_m + i\eta} \right) + \text{c.c.} \right], \quad (20)$$

where c.c. represents the complex conjugate of the first term within the square brackets. The sum of the diagrams of Fig. 1 can be summarized as the resonance X-ray absorption intensity,

$$I^r(\omega) = 2\pi \sum_{np} |f_p|\Delta|g_n\rangle + i f_p|X(\omega)|g_n\rangle|^2 \delta(\omega + \varepsilon_n - \varepsilon_p), \quad (21)$$

where the vertex operator $X(\omega)$ is given by

$$\begin{aligned}
 X(x, x'; \omega) &= \int (d\varepsilon/2\pi) dx_1 G(x, x_1; \varepsilon) \Delta(x_1) G(x_1, x'; \omega + \varepsilon) \\
 &\quad \times v(\mathbf{r} - \mathbf{r}') \\
 &= i \sum_{mq} \left[\frac{f_q(x) g_m^*(x') \langle f_q | \Delta | g_m \rangle}{\omega - \varepsilon_q + \varepsilon_m + i\eta} \right. \\
 &\quad \left. - \frac{g_m(x) f_q^*(x') \langle g_m | \Delta | f_q \rangle}{\omega - \varepsilon_m + \varepsilon_q - i\eta} \right] v(\mathbf{r} - \mathbf{r}') \quad (22)
 \end{aligned}$$

and

$$\begin{aligned}
 X(x, x'; \omega)^* &= \int (d\varepsilon/2\pi) dx_1 \tilde{G}(x', x_1; \omega + \varepsilon) \Delta^*(x_1) \\
 &\quad \times \tilde{G}(x_1, x; \varepsilon) v(\mathbf{r} - \mathbf{r}'). \quad (23)
 \end{aligned}$$

We can replace the bare Coulomb interaction v by the screened Coulomb interaction W if we want more accurate calculations. Equation (20) plays an important role when one of the energy denominators is close to zero. The X-ray photon energy ω exceeds the threshold of the shallow core φ_c and it can be close to the threshold of the deeper core φ_d ; $\omega \simeq -\varepsilon_m$. Now we have an approximate expression for the Dyson orbital, $g_m(x) \simeq \varphi_d(x) S_m^d$. The intrinsic amplitude S_m^d will be defined below. The particle Dyson orbital f_q can be localized, delocalized or even unbounded (scattering). The largest contribution to the two-electron integrals, such as $\langle f_q f_p | g_n g_m \rangle$, is expected for localized f_q . In this case it can be assumed that $\varepsilon_q \simeq 0$. From this consideration, the second term of $X(\omega)$ in equation (22) is found to be negligibly small in comparison with the first term because of the large energy denominator. Near resonance, $\omega \simeq \varepsilon_q - \varepsilon_m$, the infinitesimal η can be replaced by finite $\Gamma > 0$ by use of the standard technique [see for example, an excellent article by Almladh & Hedin (1983)].

From the above considerations, the resonance X-ray absorption intensity can be written near the resonance energy $\omega \simeq \varepsilon_m$:

$$\begin{aligned}
 I^r(\omega) &\simeq 2\pi \sum_{np} \left| \langle f_p | \Delta | g_n \rangle + \sum_q \frac{\langle f_p g_m | f_q g_n \rangle \langle f_q | \Delta | g_m \rangle}{\omega - \varepsilon_q + \varepsilon_m + i\Gamma} \right|^2 \\
 &\quad \times \delta(\omega + \varepsilon_n - \varepsilon_p). \quad (24)
 \end{aligned}$$

Near the threshold of the deeper core φ_d , the main contribution of course comes from $|\langle f_p | \Delta | \varphi_d \rangle|^2$. In addition, we expect a finite but small contribution from the tail of the shallow-core X-ray absorption intensity. Furthermore, we can expect the resonance contribution near the deeper-core threshold in some special cases. For simplicity, we only consider the two cores: the shallow core φ_c and the deep core φ_d . In this case, the X-ray absorption intensity near the threshold of the deep core is obtained by

$$\begin{aligned}
 I^r(\omega) &\simeq 2\pi \sum_{np} |\langle f_p | \Delta | \varphi_d \rangle|^2 |S_n^d|^2 \delta(\omega + \varepsilon_n^d - \varepsilon_p) \\
 &\quad + 2\pi \sum_{np} \left| \langle f_p | \Delta | \varphi_c \rangle + \sum_q \frac{\langle f_p \varphi_d | f_q \varphi_c \rangle \langle f_q | \Delta | \varphi_d \rangle}{\omega - \varepsilon_q + \varepsilon_0^d + i\Gamma} \right|^2 \\
 &\quad \times |S_n^c|^2 \delta(\omega + \varepsilon_n^c - \varepsilon_p), \quad (25)
 \end{aligned}$$

where S_n^d is the intrinsic (shake-off or shake-up) amplitude associated with the deep-core excitation given by use of the annihilation operator d of the deep-core state φ_d ,

$$S_n^d = \langle n, N-1 | d | 0, N \rangle. \quad (26)$$

In the second term of equation (25), we take only one channel $m = 0$ for the intermediate state and use an approximation $|S_0^d|^2 \simeq 1$ to simplify the formula. The first term of (25) represents the edge jump at the φ_d excitation threshold, while the second term shows the Fano shape.

Let us study the resonance contribution to the X-ray absorption intensity by use of equation (25). The first term for the isolated atom is approximately given by equation (27) for the threshold region of the deep core (Agarwal, 1991):

$$I^d(\omega) \simeq C \{ (1/\pi) \arctan[(\omega - \omega_0)/(\Gamma/2)] + 1/2 \}. \quad (27)$$

For polyatomic systems, multiple-scattering effects give rise to large structures (XANES) on $I^d(\omega)$. For simplicity, we neglect these effects here. The resonance term associated with the excitation from the shallow core, c , is given by (Almladh & Hedin, 1983)

$$I^c(\omega) = A(\omega + B)^2 / [\omega^2 + (\Gamma'/2)^2]. \quad (28)$$

The total X-ray absorption intensity near the deeper-core threshold is thus given by

$$I^r(\omega) = I^c(\omega) + I^d(\omega). \quad (29)$$

Fig. 2 represents the result of a model calculation with parameters $C/A = 10$, $B = 1$, $\Gamma = \Gamma' = 2$ and $\omega_0 = -2.5$. The resonance absorption $I^c(\omega)$ shows the Fano shape and the total absorption spectra reveal a prominent structure arising from the resonance effects, not from the one-electron transition. Of course, in the case $\omega_0 \simeq -B$ or $C/A \gg 1$, no such prominent structure is observed near the threshold.

Fig. 3 also shows the calculated result with the same parameters for B , Γ and Γ' , but with different values of C/A and ω_0 : $C/A = 20$ and $\omega_0 = -0.5$. In this case, the resonance effects do not give striking structures compared with Fig. 2, as expected.

Sato *et al.* (1999) have reported an interesting result for resonant photoemission and X-ray absorption spectra produced by excitation from the Mn $2p$ core level in NiAs-type MnTe. The Mn $2p$ X-ray absorption spectra are dominated by Mn $2p$ - $3d$ resonance excitation processes. So far, however, we have no reliable experimental data to perform a fit according to equation (29).

Typically, resonant photoemission spectra are observed when intra-atomic processes play a dominant role (Almladh & Hedin, 1983), whereas recent studies demonstrate the importance of inter-atomic resonance processes (Kay *et al.*, 1998). The latter processes can also contribute to the resonance peak in XAFS spectra near the threshold. For example, we can expect the resonance peak from the O $1s$ excitation near the Mn $2p$ threshold for MnO, which can be mislead us to some incorrect conclusions based on the simple intra-atomic $2p \rightarrow 3d$ transition interpretation. This effect can raise questions

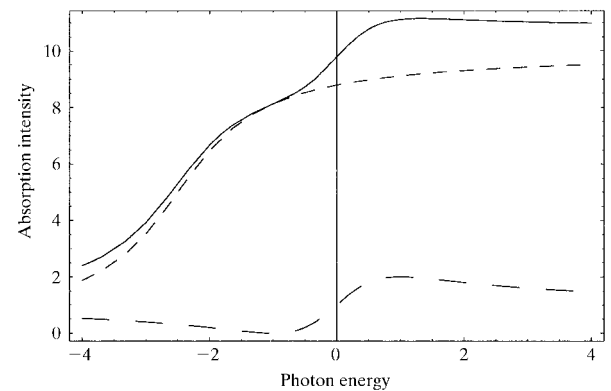


Figure 2

Near-edge X-ray absorption spectra in the deep-core region. The continuum absorption spectrum for an isolated atom for a deep core φ_d given by equation (27) (short dashes), the resonance spectrum for a shallow core φ_c given by equation (28) (long dashes) and the sum of the two contributions (full line) are presented. The parameters used here are $C/A = 10$, $B = 1$, $\Gamma = \Gamma' = 2$ and $\omega_0 = -2.5$.

regarding the interpretation of X-ray magnetic circular dichroism (XMCD) spectra at the threshold of a light element such as C, N or O, which have very small spin-orbit interactions. If nearby transition elements can contribute to the inter-atomic resonance, the XMCD can be pronounced by use of the spin-orbit interactions of the transition metal, not of the light elements.

In cases where strong resonance photoemission is observed, we should analyse the near-edge spectra carefully.

5. Extrinsic and intrinsic loss effects

Loss structures observed in XAFS spectra are usually analysed without considering the interference term. In this approximation, we can expect an abrupt jump of the absorption intensity at the threshold of the additional excitation of outer electrons (Rehr *et al.*, 1978). However, such structures have not been observed in XANES spectra. In the case of XPS (X-ray photoemission spectroscopy) spectra, the importance of the interference between intrinsic and extrinsic losses has been well established from experimental results for plasmon losses. For excitation by low-energy photons, the spectra are featureless and are lost in the background; the two losses are cancelled at the threshold because of destructive quantum interference. A similar situation can be expected for XAFS because the X-ray absorption intensity formulae are obtained by averaging over all possible final states for the XPS intensity formulae.

To determine the explicit formula for the diagrams in Figs. 4(a) and 4(b), we should calculate the spectral representation of the screened Coulomb interaction $W^>$ and $W^<$:

$$W^>(x, x'; \omega) = 2\pi i \sum_{m>0} v_m^*(x) v_m(x') \delta(\omega - \omega_m), \quad (30)$$

where the fluctuation potential $v_m(x)$ is defined by use of bare Coulomb potential v ,

$$v_m(x) = \int v(x - x') \langle m | \rho(x') | 0 \rangle dx'. \quad (31)$$

$W^<$ is related to $W^>$ by

$$W^>(x, x'; \omega) = W^<(x', x; -\omega). \quad (32)$$

Using these expressions, Fig. 4(a) gives the X-ray absorption intensity formula as

$$\begin{aligned} I(\omega)_a = & - \sum_{ml} \int dx_1 dx_2 dx_3 dx_4 \Delta^*(x_1) \tilde{G}(x_3, x_1; \varepsilon_l - \omega_m) \\ & \times g_l(x_2) \Delta(x_3) g_l^*(x_3) G(x_4, x_2; \omega + \varepsilon_l) \\ & \times G^>(x_1, x_4; \omega - \omega_m) v_m^*(x_3) v_m(x_4). \end{aligned} \quad (33)$$

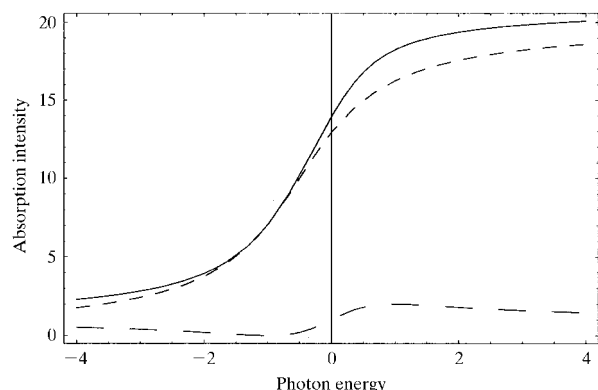


Figure 3
Same as Fig. 2, except that $C/A = 20$ and $\omega_0 = -0.5$.

In these loss diagrams, $W^>$ and $W^<$ include real loss processes, while W and \tilde{W} include virtual loss processes associated with resonance effects, as discussed in the previous section. As we are considering the core-excitation process, $\tilde{G}(\varepsilon_l - \omega_n)$ can be approximated by the hole part because the energy denominator of the particle part is large:

$$\tilde{G}(x, x'; \varepsilon_l - \omega_n) \simeq - \sum_n \frac{g_n(x) g_n^*(x')}{\varepsilon_l - \omega_m - \varepsilon_n + i\eta}. \quad (34)$$

This approximation greatly simplifies the integral over x_3 :

$$\int g_l^*(x_3) v_m^*(x_3) \tilde{G}(x_3, x_1; \varepsilon_l - \omega_m) dx_3 \simeq S_l^* \phi_c^*(x_1) \langle c | v_m | c \rangle / \omega_m. \quad (35)$$

The amplitude of the intrinsic loss S_m is related to the fluctuation potential v_m (Bardyszewski & Hedin, 1985; Fujikawa, 1993):

$$S_m = - \langle c | v_m | c \rangle / \omega_m. \quad (36)$$

The hole part of $G(\omega + \varepsilon_l)$ including g_l is small because of the large energy denominator; thus we can obtain the approximate relation

$$G(\omega + \varepsilon_l) \simeq G_{sc}(\omega + \varepsilon_l).$$

We can also employ the approximation $G^> \simeq 2G^r$ as used for equation (13) in the Im operation. These approximations lead to the X-ray absorption intensity

$$I(\omega)_a \simeq -2 \sum_{m>0} \text{Im}[\langle c | \Delta^* g(\varepsilon - \omega_m) v_m g(\varepsilon) \Delta | c \rangle S_m^* S_0], \quad (37)$$

where ε is the kinetic energy of the photoelectrons [$= \omega + \varepsilon_0 = \omega + E_0(N) - E_0(N - 1)$]. Here the retarded Green's function G^r is replaced by the damping scattering Green's function $g(\varepsilon)$ under the influence of the optical potential Σ^r .

Fig. 4(b) gives the same X-ray absorption intensity as Fig. 4(a). These diagrams describe the interference effects between the processes of intrinsic and extrinsic loss.

Near the threshold of the loss channel m , the interference term $-4\text{Im}[\langle c | \Delta^* g(\varepsilon - \omega_m) v_m g(\varepsilon) \Delta | c \rangle S_m^* S_0]$ is cancelled by the intrinsic-loss term $-2|S_m|^2 \text{Im}[\langle c | \Delta^* g(\varepsilon - \omega_m) \Delta | c \rangle]$ as discussed previously (Fujikawa, 1993). A similar discussion based on the quasi-boson approximation leads to the same conclusion (Hedin, 1989; Rehr *et al.*, 1997).

6. Other first-order terms

From the second term of equation (2), PWP , we have four different terms, $\tilde{P}_0 \tilde{W} P_0^>$, $P_0^> W P_0$, $\tilde{P}_0 W^> P_0$ and $P_0^> W^< P_0^>$, where P_0 is the skeleton bubble as shown in Fig. 1(a). All of them include $W(\omega)$, which is not important for high-energy excitation, *e.g.* $\omega \gg \omega_p$ (plasmon energy). These terms correspond to screening of the radiation field (Feibelman & Eastman, 1974). Of course, these terms could be important for valence excitation.

Within this theoretical framework, electron-phonon interactions can be discussed by use of Keldysh diagrams similar to those of Fig. 4, but with the screened Coulomb lines replaced by phonon lines

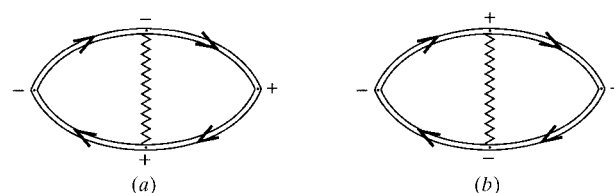


Figure 4
The skeleton Keldysh diagrams for loss processes (a) and (b), describing the interference between the intrinsic and the extrinsic losses.

(Hedin & Lundqvist, 1969). So far such effects have not been discussed. Note that the Debye–Waller and Franck–Condon factors do not enter XAFS formulae by use of the electron–phonon interaction.

7. Concluding remarks

Approaches based on the non-equilibrium Keldysh–Green function represent a ‘natural language’ with which to interpret XAFS spectra, both at $T = 0$ and at finite temperature. The first-order terms including the screened Coulomb interaction $W^>$ or $W^<$ in the skeleton expansion describe the interference processes of extrinsic–intrinsic loss, whereas those including W or \tilde{W} describe the resonance effects.

The author is grateful to Dr T. Konishi for valuable discussions, in particular for the discussion of the resonance effects.

References

Agarwal, B. K. (1991). *X-ray Spectroscopy*, 2nd ed. New York: Springer.

- Almbladh, C.-O. & Hedin, L. (1983). *Handbook on Synchrotron Radiation*, Vol. 1b, edited by E. E. Koch, pp. 607–904. Amsterdam: North-Holland.
- Bardyszewski, W. & Hedin, L. (1985). *Phys. Scr.* **32**, 439–450.
- Binsted, N. & Hasnain, S. S. (1996). *J. Synchrotron Rad.* **3**, 185–196.
- Feibelman, P. J. & Eastman, D. E. (1974). *Phys. Rev. B*, **10**, 4932–4947.
- Fujikawa, T. (1993). *J. Phys. Soc. Jpn.* **62**, 2155–2165.
- Fujikawa, T. (1996a). *J. Phys. Soc. Jpn.* **65**, 87–94.
- Fujikawa, T. (1996b). *J. Elect. Spectrosc.* **79**, 25–28.
- Fujikawa, T. (1999). *J. Phys. Soc. Jpn.* **68**, 2444–2456.
- Hedin, L. (1989). *Physica B*, **158**, 344–346.
- Hedin, L. & Lundqvist, S. (1969). *Solid State Physics*, Vol. 23, edited by F. Seitz, D. Turnbull & H. Ehrenreich, pp. 1–181. New York: Academic Press.
- Kay, A., Arenholz, E., Mun, S., Garcia de Abajo, F. J., Fadley, C. S., Denecke, R., Hussain, Z. & Van Hove, M. A. (1998). *Science*, **281**, 679–683.
- Lee, P. A. & Pendry, J. B. (1975). *Phys. Rev. B*, **11**, 2795–2811.
- Mahan, G. D. (1990). *Many-Particle Physics*, 2nd ed. Oxford: Plenum.
- Rehr, J. J., Bardyszewski, W. & Hedin, L. (1997). *J. Phys. IV (France)*, **7(C2)**, 97–98.
- Rehr, J. J., Mustre de Leon, J., Zabinsky, S. I. & Albers, R. C. (1991). *J. Am. Chem. Soc.* **113**, 5135–5140.
- Rehr, J. J., Stern, E. A., Martin, R. L. & Davidson, E. R. (1978). *Phys. Rev. B*, **17**, 560–565.
- Sato, H., Tanaka, A., Furuta, A., Senba, S., Okuda, H., Mimura, K., Nakatake, M., Ueda, Y., Taniguchi, M. & Jo, T. (1999). *J. Phys. Soc. Jpn.* **68**, 2132–2138.